Proceedings of the 5th WSEAS International Conference on Applied Computer Science, Hangzhou, China, April 16-18, 2006 (pp422-427)

Biometric authentication using digital retinal images

M. ORTEGA, C.MARIÑO, M.G.PENEDO, M.BLANCO, F.GONZ ÁLEZ†
Grupo de Visión Artificial y Reconocimiento de Patrones
University of A Coruña
Campus de Elviña s/n, A Coruña, 15071
†University of Santiago de Compostela
†School of Medicine andComplejo Hospitalario Universitario of Santiago, 15782 Santiago de Compostela
SPAIN

Abstract: In this work an efficient method for the identity verification of persons based on matching digital retinal images is introduced. The matching process works by extracting a set of feature points and registering them to measure the degree of similarity between the input images. The feature points are the ridge endings and ridge bifurcations from vessels obtained from a crease model of the retinal vessels. The method is developed and tested to obtain a good set of feature points. Then, pairs of sets will be matched in order to get an accurate and reliable similarity measure for the authentication procedure.

Key–Words: Biometric authentication, registration, similarity measure, optic disc.

1 Introduction

Reliable authentication of persons is a growing demanding service in many fields, not only in police or military environments, but also in civilian applications, such as access control or financial transactions. Traditional authentication systems are based on knowledge (a password, a pin) or possession (a card, a key). But these systems are not reliable enough for many environments, due to their common inability to differentiate between a true authorized user and an user who fraudulently acquired the privilege of the authorized user. A solution to these problems has been found in the biometric based authentication technologies. A biometric system is a pattern recognition system that establishes the authenticity of a specific physiological or behavioral characteristic. Identification can be in the form of authentication (identity verification), verification (authenticating a claimed identity) or recognition (determination of an identity from a database of known people, this is, determining who a person is without knowledge of his/her name).

Many authentication technologies can be found in the literature [1–4]. But, nowadays, the most of the efforts in authentication systems tend to develop more secure environments, where it is harder, or ideally, impossible, to create a copy of the properties used by the system do discriminate between authorized and unauthorized individuals.

This paper proposes a biometric system for authentication that uses the blood vessel pattern. This is a unique pattern in each individual and it is almost impossible to forge that pattern in a false individual. Of course, the pattern does not change through the individual's life, unless a pathology appears in the eye. This biometric parameter has already shown to be a good choice in [5, 6]. In this paper, a more compact representation of the retinal vessel tree is employed.

Classical fingerprint authentication methods rely on representing the two most prominent structures: ridge endings and and ridge bifurcations [1, 7]. In this work, the same landmarks are extracted and employed as the template that characterizes an individual in the system.

In a first stage of our method, the extraction of the features to use as anatomical landmarks takes place. In our case, these features will be the ridge endings and ridge bifurcations of the whole retinal vessel tree extracted from a set of crest and valley lines. This technique is very similar to the methodology used in the fingerprint based authentication [8]. Once that pattern has been obtained, it is stored in a database of authorized people. When a person needs to be authenticated, the acquired image is processed to extract the set of feature points, and a registration method aligns these points with the pattern stored from this individual. For a review of medical image registration methods see [9]). The registration process is necessary due to inevitable eye movements that must be corrected prior to the application of quantitative analysis. Once the images are aligned, a similarity measure can be computed. If this measure is higher than a

given threshold, the individual is accepted, otherwise the individual is rejected.

2 Feature points extraction

As stated above, the biometric parameter used by the proposed system is the whole retinal vessel tree, extracted from digital retinal images. In order to reduce the computational time, only a set of points is extracted and used to register the images and perform the authentication test, without a loss of accuracy or reliability. The point extraction is performed in three steps: (1) Creases extraction, (2) optic nerve extraction and (3) feature point extraction. Each stage is described in the following sections.

2.1 Creases extraction

Vessels are reliable landmarks in retinal images because they are almost rigid structures and they appear in all modalities. Moreover, they can be thought of as creases (ridges or valleys) when images are seen as landscapes.

Among the many definitions of a crease, the one based on level set extrinsic curvature (LSEC), has useful invariance properties. Given a function $L : \mathbf{R}^d \rightarrow \mathbf{R}$, the level set for a constant l consists of the set of points $\{\mathbf{x}|L(\mathbf{x}) = l\}$. For $2D$ images, L can be considered as a topographic relief or landscape and the level sets as its level curves. Negative minima of the level curve curvature κ, level by level, form valley curves, and positive maxima form ridge curves.

However, the usual discretization of LSEC is ill–defined in a number of cases, giving rise to unexpected discontinuities at the center of elongated objects. Due to this, we have employed the $MLSEC-ST$ operator, defined in [10] and [11] for 3–D landmark extraction of CT and MRI volumes. This alternative definition is based on the divergence of the normalized vector field $\bar{\mathbf{w}}$:

$$\kappa = -\mathrm{div}(\bar{\mathbf{w}}) \tag{1}$$

The creaseness measure κ can still be improved by pre–filtering the image gradient vector field in order to increase the degree of attraction/repulsion at ridge–like/valley–like creases as this is what κ actually measures. This can be done by the following structure tensor analysis: (1) Compute the gradient vector field $\mathbf{w}$ and the structure tensor field $\mathbf{M}$ $\mathbf{M}(\mathbf{x};\sigma_{\mathrm{I}}) = G(\mathbf{x};\sigma_{\mathrm{I}}) * (\mathbf{w}(\mathbf{x}) \cdot \mathbf{w}(\mathbf{x})^{\mathrm{t}})$, where $*$ is the element–wise convolution of matrix $\mathbf{w}(\mathbf{x}) \cdot \mathbf{w}(\mathbf{x})^{\mathrm{t}}$ with the Gaussian window $G(\mathbf{x};\sigma_{\mathrm{I}})$. (2) Perform the eigenvalue analysis of $\mathbf{M}$. The normalized eigenvector $\mathbf{w}'$ corresponding to the highest eigenvalue gives the predominant gradient orientation. In the structure tensor analysis, opposite directions are equally treated. Thus, to recover the direction $\mathbf{w}'$ is located in the same quadrant in 2–d, or octant in 3–d, as $\mathbf{w}$. Then, the new vector field $\tilde{\mathbf{w}}$ and the creaseness measure $\tilde{\kappa}_d$ are computed as:

$$\tilde{\mathbf{w}} = \mathrm{sign}(\mathbf{w}'^{\mathrm{t}}\mathbf{w})\mathbf{w}' \tag{2}$$

$$\tilde{\kappa} = -\mathrm{div}(\tilde{\mathbf{w}}) \tag{3}$$

Figure 1 left, shows the result of the creases extraction algorithm.

2.2 Optic disc extraction

The optic disc is the brightest area in the digital retinal images, with an almost circular shape. It is the entrance region of the vessels and its detection is very important as it works as a landmark for the other features in the retinal image. To determine the position of the optic disc, a two-stage algorithm is used: in the first stage, the area (region of interest) where the optic disc is located is determined (Figure 1, center). Then, the fuzzy circular Hough transform is applied to the edges of the region in order to extract the optic disc. The fuzzy circular Hough transform might not extract the disc due to the fact that there are vessels inside the optic disc. In order to eliminate the circles belonging to vessel edges, the vessel edge points are eliminated. To this end, an automatic vessel extraction is performed by the algorithm described in section 2.1. Once the crease image in the region of interest is computed by the previous process, the edge vessels are removed. If an edge point (x_i, y_i) belongs to a vessel, an $w_a \times w_b$ neighborhood window centered at the crease point is considered in the edge image. If the direction of an edge point in the window is analogous to the direction of the crease point, this edge point is removed. Figure 1,right, depicts the results obtained by this algorithm on a retinal image [12].

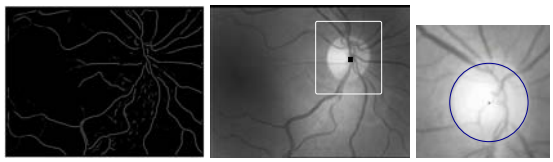

Fig 1: Left: result of the creases extraction. Center: result of the region of interest computation. Right: result of the optic disc segmentation process.

2.3 Point extraction

Once the creases image and the optic disc position have been computed, the feature point search stage be-

gins. As already stated, the feature points are the ridge endings and bifurcations of the creases. In this paper, the term 'bifurcation' refers to any of both kind of feature points since they are all extracted in the same way.

To make an efficient approach to the problem, instead of tracking the segments trying to find feature points along them in a given radius, only the environment around the creases segment extremes will be analyzed.

Still another problem must be solved prior to the feature point extraction: the creases segments from the same vessel sometimes appear as different segments. So, relationships between segments will be established in order to build the retinal vessel tree. The two kind of relationships to take into account are unions (a segment is the continuation of another one, belonging both to the same vessel) and bifurcations (a segment, coming out of another segment, starts a new vessel).

Our feature points extraction algorithm has the following stages: (1) Segment detection, (2) segment union detection, (3) segment bifurcation candidates detection and finally, (4) feature point set extraction.

In order to obtain the segments in the image, a simple but very efficient algorithm is used. The entire creases image is tracked and when a non-zero pixel is found, the disposition of its four possible neighbors is analyzed (since the image tracking is from left to right and from top to bottom, upper neighbors and left neighbor are always zero), and in any of the 8 possible cases the segment pixels are accordingly tracked.

As later we will have to deal with the segments directions, each point is assigned a predecessor and a successor, to specify its direction. Also, the endings are accordingly labelled as the start and the end of the segment. If the set directions are not right, they will be corrected in a next stage. The purpose of establishing these directions at this stage is to have a reference direction to use in further analysis.

The unions between segments are important in order to build the whole vessel tree, because they allow to continue the vessels and propagate the correct direction to the bifurcation segment candidates.

A union is a relationship between two endpoints of different segments. A union is accepted as right when the endpoints are close to each other, and, of course, a segment represents the continuation of the other. This means that they must have similar orientations and the connection between them should be smooth.

From the experiments run, it was observed that connecting both segments through a straight line is enough to determine the likelihood of that union to belong to the same crease, as depicted in Figure 2. The closer to 180° the angles of the segments are, the smoother the union is. An angle threshold θ is necessary to discard wrong unions. Values of θ close to 135° deliver good results in the vast majority of the cases.

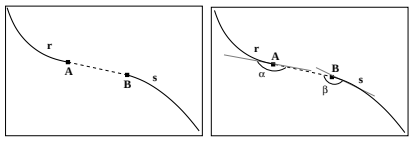

Fig 2: Left: Union of creases segments r and s. Right: the angles between the new segment $\overline{AB}$ and the creases segments r (α) and s (β) are near πrad so they are above the required threshold ($\frac{3}{4}\pi$) and the union is finally accepted.

In the segments obtained via the crease extraction, a bifurcation point is composed of a segment endpoint and another segment point where the first segment really starts from. Again, as in the union detection process, each segment endpoint is analyzed searching this time for the possible segment candidates (if any) to form a bifurcation with it. The process is as follows (Figure 3 right): (1) Compute the endpoint direction. (2) Extend the segment in that direction a fixed length l_{max}. (3) Analyze the points in and nearby the prolongation segment to find candidate segments. (4) If a point of a different segment is found, compute the angle (ϕ) associated to that bifurcation, defined by the direction of this point and the extreme direction from step (1).

To avoid undefined prolongation of the segments, a new parameter l_{max} is inserted in the model. If it follows that $l <= l_{max}$, the segments will be joined and a bifurcation will be detected, being l the distance from the endpoint of the segment to the other segment. Otherwise two ridge endings will be found.

Once a segment point is found, the angle ϕ associated to the bifurcation is computed. This angle is obtained as the difference between both segment directions of the involved points. Note that depending on the direction of the detected segment, this angle can be ϕ or π-ϕ (radians). Figure 3, center, illustrates this dichotomy.

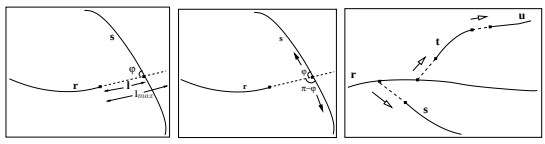

Fig 3: Left: Bifurcation between segment r and s. The endpoint of r is prolongated a distance l_{max} and eventually a point of segment s is found. Center: Illustration of the angle variation depending on the segment direction considered. Right: Segment directions are extended through bifurcations (segment r propagates to s and t) and unions (segments t to u).

The direction will determine if this candidate bifurcation is finally accepted or discarded. In the last stage, final segment directions are established allowing to decide whether the feature point candidates are accepted or rejected. Due to this, a value associated to each candidate is stored at this stage, indicating the direction of the segment.

In order to determine the right directions of the segments, the whole retinal vessel tree is built from the segments starting at the optic disc and propagating the directions through the bifurcations and junctions.

As the location of the optic disc is known, a circle around the disc can be drawn. Tracking this circle the segments that intersect with the circle will be obtained. These are the initial segments of the process. The right direction of these segments is set as the starting endpoint in contact with the optic disc) and then, for each one of them, bifurcation candidates are analyzed. If the direction of the candidate branch to be accepted is adequate, the bifurcation is accepted and the direction is propagated to the other segment forming that bifurcation. Recursively, directions are propagated through bifurcations and unions. An example is shown in Figure 3, right.

Once the recursive process finishes, the whole retinal vessel tree is built and the bifurcation points characterizing the image are determined (Figure 4).

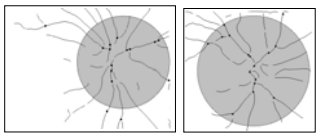

Fig 4: Example of the feature points extracted in two crease images. Gray area represents the zone around the optic disc where points are stored.

Due to the poor quality of the image in some areas or the crease extraction process, some segments might be separated from the tree segments. If the direction of some of these segments is necessary to determine the acceptance or rejection of some bifurcation candidate, following heuristic is applied: the vessels begin at the optic disc, so the starting point will probably be closer to it than the ending one.

Some ”spurious” segments might appear in the image, usually in regions where the contrast is low. Due to this, only the points around the optic disc in a given radius r will be considered. So, the feature points set is centered in the optic disc, which makes easier and more efficient the registration and matching process explained in the following section. Figure 4 shows some feature point sets obtained from two different images inside of the circumference of radius r (gray area in Figure 4).

3 Registration and Matching

From the previously proposed feature point set extraction algorithm, a point pattern matching algorithm has been developed. The algorithm receives two feature point sets as input, and produces a matching value expressing the similarity between the two retinal images (the ”reference image” stored in the database of authorized users and the ”candidate image”). This value will determine if the candidate image is accepted or rejected.

Two retinal images from the same person obtained at different moments will probably be different because of the eye movements.The transformation considered in this work is the Similarity Transformation (ST), which is a special case of the Global Affine Transformation (GAT). ST can model translation, rotation and isotropic scaling using 4 parameters: $(\Delta x,\Delta y,S,\theta)$ to model the translation in x-axis, the translation in y-axis, the scaling and the rotation respectively. The ST works fine with this kind of images where the rotation angle is moderate. It has also been observed that the scaling, due to eye proximity to the camera, is nearly constant for all the images. Also, the rotations are very slight as the eye orientation when facing the camera is very similar. Under these circumstances, the ST model appears to be very suitable, with the additional benefit that it is a very efficient model compared to the higher-level ones.

The ultimate goal is to achieve a final value indicating the similarity between the two feature points set, in order to decide about the acceptance or the rejection of the hypothesis that both images correspond to the same individual. To develop this task the matching pairings between both images must be determined. A transformation has to be applied to the candidate image in order to register its feature points with respect to the corresponding points in the reference image. The set of possible transformations is built based on some restrictions and a matching process is performed for each one of these. The transformation with the highest matching score will be accepted as the best transformation.

To obtain the four parameters of a concrete ST, three pairs of feature points between the reference and candidate images are considered. The set of possible transformations is obtained by building an initial set similar to that described in [13].Being M the total number of feature points in the reference image and N the total number of points in the candidate one, the size of the set T of possible transformations is computed using Equation 4.

$$T = \frac{(M^2 - M)(N^2 - N)}{2} \tag{4}$$

Since T is a high number of transformations, some restrictions must be applied in order to reduce it. The spatial information of the optic disc in both images can help us to significantly reduce the size of T. Unfortunately, the location of the disc is not precise enough to consider it a control point to the transformation. But, its location can be considered precise enough to restrict that two points, A and A', from the reference and candidate images, respectively, can only match if the distance to their respective optic discs is very similar. This is true as the scaling factor is considered to be approximately 1 in the images and the ST respects the shape of image. The parameter d_{max} represents that maximum accepted difference. Equation 5 formalizes this restriction.

$$distance(A,O) - distance(A',O') < d_{max} \quad (5)$$

where O and O' are the estimated optic disc location in the reference and candidate images, respectively. With this technique, the number of possible matches greatly decrease and so the set of possible transformations. The mean percentage of deleted transformations is around 80-90%.

The matching algorithm proposed here is based on that described in [4]. In order to check feature points, a similarity value (S) is defined which indicates how similar two points are. The distance between these two points will be used to compute that value. For two points A and B, this value is defined by Equation 6

$$S(A,B) = 1 - \frac{distance(A,B)}{D} \quad (6)$$

where D stands for the maximum distance allowed for those points to be considered a possible match. If $distance(A,B) > D$ then $S = 0$.

In some cases,two points C_1, C_2 could have both a good value of similarity with one point R in the reference image. This happens because C_1 and C_2 are close to each other in the candidate image. To identify the most suitable matching pair, the possibility of correspondence is defined comparing the similarity value between those points to the rest of similarity values of each one of them by means of Equation 7.

$$P(A_i,B_j) = \frac{S(A_i,B_j)^2}{\left(\sum_{i'=1}^{M} S(A_{i'},B_j) + \sum_{j'=1}^{N} S(A_i,B_{j'}) - S(A_i,B_j)\right)} \quad (7)$$

A $M \times N$ matrix Q is constructed such that position (i,j) holds $P(i,j)$. If the similarity value is 0, the possibility value is also 0. This means that only valid matchings will have a non-zero value in Q. The desired set C of matching feature points is obtained from P using a greedy algorithm. The element inserted in C, (i,j), is the position in Q where the maximum value is stored. Then, to prevent the selection of the same point in one of the images again, the row (i) and the column(j) associated to that pair are set to 0. The algorithm finishes when no more non-zero elements can be picked from Q.

Finally, the matching value that measures the similarity between both points sets is computed by mens of Equation 8.

$$\frac{1}{\sqrt{MN}} \sum_{(i,c)\in C} S(A_i,B_j) \quad (8)$$

where M and N are the number of points of both feature point sets.

4 Method Validation and Results

Images employed in these experiments were acquired during a period of 15 months in different centers of the University Hospital of Santiago de Compostela (CHUS), and with the same camera, a Cannon CR6-45NM Non-Mydriatic Retinal Camera, with a resolution of 768x584 pixels. Although the camera originally capture color images, a conversion to gray-level images (with 256 gray levels) was performed prior to the storage in the database, since color does not provide any useful information.

In order to tune the parameters of the process and to check its suitability to perform the authentication task, an experiment was performed. A set of 16 images (4 images from 2 persons and 12 images from 12 persons) is evaluated by the system. Good feature extraction and matching parameters were obtained with this experiment where the positive cases showed values above 0.5 and the negative cases under 0.25.

In this test, the matching score for the Cartesian product of the 12 images was computed. The diagonal of this Cartesian product consists of 1.0 values, as they correspond to the evaluation of an image with itself. The rest of evaluations proved that values under 0.32 were always obtained from images belonging to different individuals, while the values over 0.5 were from images belonging to the same individual.

The experiment demonstrated that, if the threshold is over 0.32, the false positive rate is always null, but it increases exponentially as the threshold value goes down from 0.32 to 0. Thus, when the threshold is over 0, the percentage of false positives is not over 0.9. Also, with threshold values below 0.5 the rate of false positives is always null. As the threshold

increases from that value, the rate of false positives increases, leading eventually to the total rejection. Taking all these results into account, when the threshold is between 0.32 and 0.5, the effectiveness of the system is 100% as it is able to find which images belong to the same person in the test images set.

5 Conclusions and future work

In this work a novel identity verification method has been introduced. To get the set of feature points, a combination of a creases-based extraction and an optic disc location algorithm is used. After that, a recursive algorithm gets the point features by tracking the creases from the localized optic disc. This procedure is performed in an area determined by the radius of the optic disc and an concentric circle of radius r. Finally, a registration process is necessary in order to match the reference image from the database and the acquired image. With the images aligned, it is possible to measure the similarity by means of a metric.

The main parameters of the process and their final values are: the maximum angle allowed between a union segment and both creases segments to accept the union (θ in Figure 3, left): $\frac{3}{4}\pi$ rad. The length of the prolongation from a segment endpoint to find the possible bifurcations (l_{max}): 25 pixels. The radius of the area surrounding the optic disc and containing the feature points to be stored for that image (r): 250 pixels. And finally the maximum difference between the distances of two feature points in candidate and reference images to their respective optic discs to be considered a possible pairing (d_{max}): 15 pixels. These choices performed well for all the tested sequences.

The mean execution time for the authentication is of 250ms: 100ms is the cost for the feature extraction stage and 150ms for the registration and similarity measure estimation, so that the method is very well-fitted to be employed in a real authentication system.

In future work, new experiments with a higher number of images will be performed in order to determine a more accurate acceptance threshold.

Acknowledgements: This paper has been partly funded by the Xunta de Galicia through the grant contracts PGIDT04PXIC10501PN and PGIDIT03TIC10503PR.

References

[1] Jain A., Hong L., Pankanti S., and Bolle R. An Identity Authentication System Using Fingerprints. *Proc. of the IEEE*, vol. 85(9), 1997.

[2] Zunkel R. Hand Geometry Based Verification. In *BIOMETRICS:Personal Identification in Networked Society*. Kluwert Academic Publishers, 1999.

[3] Zhao W., Chellappa R., Rosenfeld A., and Phillips P. Face recognition: A literature survey. *Tech. rep.*, National Institute of Standards and Technology, 2000.

[4] Tico M. and Kuosmanen P. Fingerprint Matching Using an Orientation-Based Minutia Descriptor. *IEEE Trans. on PAMI*, vol. 25(8), 2003, pp. 1009–1014.

[5] Mariño C., Penedo M., Carreira M., and González F. Retinal angiography based authentication. *Lecture Notes in Computer Science*, vol. 2905, 2003, pp. 306–313.

[6] Mariño C., Penedo M.G., Penas M., Carreira M.J., and González F. Personal authentication using digital retinal images. *Pattern Recognition Letters*, vol. DOI 10.1007/s10044-005-0022-6, 2006.

[7] Tan X. and Bhanu B. A robust two step approach for fingerprint identification. *Pattern Recognition Letters*, vol. 24, 2003, pp. 2127–2134.

[8] Jain A., Hong L., Pankanti S., and Bolle R. An identity-authentication system using fingerprints. *Proc. of the IEEE*, vol. 85(9), 1997, pp. 1365–1388.

[9] Zitová B. and Flusser J. Image registration methods: a survey. *Image Vision and Computing*, vol. 21(11), 2003, pp. 977–1000.

[10] López A., Lloret D., Serrat J., and Villanueva J. Multilocal creasness based on the level set extrinsic curvature. *Computer Vision and Image Understanding*, vol. 77, 2000, pp. 111–144.

[11] Peña A.L., Lumbreras F., Serrat J., and Villanueva J. Evaluation of methods for ridge and valley detection. *IEEE Trans. on PAMI*, vol. 21, 1999, pp. 327–335.

[12] Blanco M., Penedo M.G., , Barreira N., Penas M., and Carreira M.J. Localization and extraction of the optic disc using the Fuzzy Circular Hough Transform, 2006. ICAISC06, Zakopane, Poland. Pending of publication.

[13] Ryan N., Heneghan C., and de Chazal P. Registration of digital retinal images using landmark correspondence by expectation maximization. *Image and Vision Computing*, vol. 22, 2004, pp. 883–898.